J Appl Electrochem (2010) 40:1933–1939
DOI 10.1007/s10800-010-0169-8

ORIGINAL PAPER

Influence of Nafion® ionomer on carbon corrosion

O. V. Cherstiouk · P. A. Simonov · V. B. Fenelonov · E. R. Savinova

Received: 28 December 2009 / Accepted: 4 July 2010 / Published online: 17 July 2010

Abstract Corrosion of the three carbon black materials which differ in their textural, sub-structural, and morphological characteristics is studied in H_2SO_4 electrolyte at 80 °C at positive polarization. Impregnation of carbon blacks with Nafion® ionomer is found to strongly affect their susceptibility to corrosion, which varies non-monotonically as a function of the Nafion® loading. Low temperature nitrogen adsorption is applied to study the distribution of the ionomer molecules in the carbon matrix.

Keywords Carbon blacks · Electrochemical corrosion · Nafion® ionomer · Vulcan XC-72 · Acetylene black · Thermal black

1 Introduction

Polymer Electrolyte Membrane Fuel Cells (PEMFCs) are considered as promising power sources for small stationary, vehicle and portable applications due to their intrinsically high thermodynamic efficiencies and environmental friendliness [1]. Corrosion stability of carbon materials, which are used as supports for fuel cell electrocatalysts, is of paramount importance for the long-term operation of PEMFCs. In 1970s–1980s corrosion of various carbon materials was extensively studied in H_3PO_4 medium in relation to the development of phosphoric acid fuel cells [2–5], and reviewed in a comprehensive treatise of Kinoshita [6]. Kinoshita and Bett [2] suggested simultaneous occurrence of two parallel anodic reactions: formation of surface oxides and evolution of CO_2, the rates of both processes decaying with time. Stonehart [3] discussed the correlation between the electrochemical properties of carbon and its d_{002} spacing, while Giordano et al. [7] examined the dependence of corrosion current on the concentration of oxygen-containing groups. Influence of Pt on carbon corrosion has also been explored [8, 9].

Recently, electrochemical corrosion of carbon attracted much attention in relation to the research and development of PEMFCs [10–16]. Various aspects were investigated and discussed, namely the influence of the temperature [3, 4, 11, 17, 18], the electrode potential [3, 13], the presence of water and the electrolyte concentration [4, 13, 19], the structure and pretreatment of carbon materials [12, 20, 21], and the catalytic effect of Pt [8, 9, 12, 16, 22]. However, to the best of our knowledge, the effect of Nafion® on the carbon corrosion has not been investigated yet. Considering that catalytic layers of PEMFCs usually contain significant (from 10 to 50%) amounts of Nafion® for improving their proton conductivity and increasing the catalyst utilization, the knowledge of its influence on the catalytic layer durability is essential. It is thus the aim of this study to study the influence of Nafion® on the corrosion of carbon blacks. Vulcan XC-72 furnace black was taken as the carbon support most widely utilized for the fabrication of the catalytic layers for PEMFCs, while acetylene black (AB) and thermal black T-900 were studied for comparison.

O. V. Cherstiouk · P. A. Simonov · V. B. Fenelonov
Boreskov Institute of Catalysis, Pr. Akademika Lavrentieva 5, 630090 Novosibirsk, Russian Federation

E. R. Savinova (✉)
l'Ecole Européenne de Chimie, Polymères et Matériaux, Université de Strasbourg, LMSPC-UMR 7515 du CNRS-UdS, 25, rue Becquerel, 67087 Strasbourg Cedex 2, France
e-mail: Elena.Savinova@unistra.fr

2 Experimental

2.1 Materials

Carbon blacks utilized in this study, Vulcan XC-72 (*Cabot*), AB (*Shawinigan*), and T-900 (*Omsk carbon black plant*, *Russia*), differ strongly in their specific surface areas (decreasing in the range Vulcan XC-72 > AB > T-900), the presence of micropores (present in Vulcan, but not in the other two carbon blacks), the dibutyl phthalate absorption (DBPA) numbers (high for Vulcan XC-72 and AB, but low for T-900), and sub-structural parameters (the interlayer spacing d_{002}, the size of graphite-like crystallites in the direction parallel (L_a) and perpendicular (L_c) to graphene layers) as represented in the Table 1.

2.2 Characterization of carbon materials

Textural characteristics of the carbon blacks, both pristine and impregnated with Nafion®, were obtained from the data on the N_2 adsorption measured at 77 K with an automatic volumetric device ASAP 2400 (*Micrometritics*). All samples were pre-treated at 373 K to a residual pressure of ca. 0.13 Pa. The values of the BET surface area A_{BET} were calculated from the adsorption isotherms at relative pressures P/P_0 of 0.05–0.2 (here P_0 is the saturation pressure). The volume of micropores V_μ accessible to nitrogen at 77 K was determined by the comparative method of Karnaukhov et al. [23], which is similar to the α_s-method of Sing and *t*-method of Lippens-de Boer [24]. The volume V_{BJH} and the surface area A_{BJH} of the pores between 1.7 and 300 nm were calculated from the desorption branches of the capillary condensation hysteresis according to the BJH model [25]. The cumulative pore volume of the pores with $d < 10$ nm ($V_{0.8}$) and with $d < 300$ nm (V_Σ) were calculated from the values of adsorption at $P/P_0 = 0.8$ and at $P/P_0 = 0.98$, respectively. The average mesopore diameters were calculated as $D_{BET} = 4\ V_\Sigma/A_{BET}$ and $D_{BJH} = 4\ V_{BJH}/A_{BJH}$ [24, 25]. The values of the surface and the volume of the pores were calculated per gram of the starting carbon material.

Sub-structural parameters of carbon materials were determined with URD6 X-ray diffractometer and Cu Kα radiation using the procedure described in reference [26].

2.3 Solutions

Solutions were prepared from Milli-Q water (18 MΩ cm), H_2SO_4 (puriss. Russia), isopropanol (puriss. Russia), Nafion® (equiv. wt. 1100, 10 wt% dispersion in water, *Aldrich*). Working electrodes were prepared by spreading an ink prepared from a mixture of carbon and corresponding amount of Nafion® on Toray TGP-H-060 paper under Ar flow. For the ink preparation, a carbon specimen was suspended in 2 ml of isopropanol:water (3:2) mixture and sonicated in an ultrasonic bath for 15 min, then an aliquot of Nafion® dispersion in water was added and the mixture was sonicated for another 15 min. The samples were dried at 105 ± 1 °C during 1.5 h in a furnace and mounted in an electrochemical cell filled with 2 M H_2SO_4 and purged with Ar. In order to ensure that the electrodes were wetted by the electrolyte, they

Table 1 Textural, sub-structural, and morphological characteristics of carbon black samples impregnated with various amounts of Nafion®

		Vulcan XC-72					Acetylene black			T-900	
Nafion® loading	mg g_C^{-1}	0.00	35.5	44.4	175	694	0.00	12.9	50.8	0.00	6.04
	mg m_C^{-2}	0.00	0.16	0.20	0.79	3.13	0.00	0.20	0.79	0.00	0.79
Surface area[a] ($m^2\ g^{-1}$)	A_{BET}	222	205	173	70.7	70.6	64.3	64.7	58.8	7.64	6.57
	A_{BJH}	89.6	96.0	91.1	90.7	70.0	46.6	47.8	45.0	5.22	5.57
Pore volume[a] ($cm^3\ g^{-1}$)	V_Σ	0.429	0.536	0.533	0.600	0.586	0.179	0.184	0.190	0.0241	0.0228
	V_{BJH}	0.356	0.475	0.487	0.626	0.585	0.164	0.168	0.179	0.0224	0.0224
	V_μ	0.026	0.018	0.008	0.00	0.00	0.00	0.00	0.00	0.00	0.00
	$V_{0.8}$	0.170	0.156	0.135	0.101	0.066	0.067	0.068	0.060	0.0075	0.0065
	$V_\Sigma - V_{0.8}$	0.259	0.380	0.398	0.499	0.520	0.112	0.116	0.130	0.0166	0.0163
	$V_{0.8} - V_\mu$	0.144	0.138	0.127	0.101	0.066	0.067	0.068	0.060	0.0075	0.0065
Mean pore size (nm)	$D_{(BET)}$	7.7	10.5	12.3	22.8	33.2	11.1	11.3	12.9	12.6	13.9
	$D_{(BJH\ des.)}$	15.9	19.8	21.4	27.5	39.4	14.1	14.8	15.9	17.2	16.1
DBP absorption (cm^3/100 g)		193					260			43	
Substructural parameters	d_{002} (Å)	3.54					3.48			3.53	
	L_c (Å)	23					37			23	
	L_a (Å)	20					29			18	

[a] The values are normalized to the mass of carbon black

were soaked in it for 16 h before the start of the measurements.

2.4 Electrochemical measurements

Electrochemical measurements were carried out in a three-electrode glass cell at 80 ± 1 °C after deaeration with Ar. The counter electrode was Pt foil and the reference was mercury sulfate electrode (MSE) Hg|Hg_2SO_4|2 M H_2SO_4 connected to the cell via Luggin capillary. Electrode potentials were controlled using Autolab PGSTAT100 potentiostat, and hereinafter are reported versus the reversible hydrogen electrode RHE ($E_{MSE} = 0.61$ V vs. RHE). Corrosion currents were measured at 1.1 V versus RHE for 1 h, and for selected samples for 72 h. Current densities were normalized to the mass of carbon. In order to exclude any artifacts arising from the oxidation of either remaining solvent molecules or impurities originating from Nafion® solution, blank experiments were performed. Toray paper was impregnated with Nafion® and the samples obtained were subjected to positive polarization at 1.1 V vs. RHE in 2 M H_2SO_4. For Vulcan XC-72, this background contribution was below 1%, while for T-900 approached 20%.

3 Results and discussion

Typical chronoamperogramms for the electrooxidation of Vulcan XC-72 and AB are shown in Fig. 1. In agreement with the literature data [2, 3], corrosion currents decay in time following t^{-n} law. The value of n is equal to 0.52 and 0.54 for Vulcan XC-72 and AB, respectively. Similar behavior was observed for T-900 (not shown) with $n = 0.64$. Long-term experiments showed no steady state current even after 72 h of the electrolysis. The discussion of the kinetics and the mechanism of the carbon corrosion being beyond the subject of this communication, we turn to the analysis of the influence of Nafion® on the carbon black oxidation.

Figure 1 shows that impregnation with Nafion® ionomer leads to remarkable changes in the oxidation currents for Vulcan XC-72 and for AB. The amplitude of the current first decreases, and then, above ca. 1 $mg_{Nafion}\ m_C^{-2}$, increases. Simultaneously, the value of n slightly decreases (from 0.52 to 0.42 for Vulcan XC-72 and from 0.54 to 0.40 for AB) and, above ca. 1 $mg_{Nafion}\ m_C^{-2}$, restores its original value. These changes are reflected also in the cyclic voltamogramms (CVs) of carbon blacks taken before and after the corrosion measurements. These are shown for Vulcan XC-72 in Fig. 2a, b. While CVs after the oxidation show a significant increase of the double layer splitting due to the formation of surface oxygen-containing groups, in particular quinine/hydroquinone, they scale with the amount of Nafion® in the same order as before the oxidation (see insets to Fig. 2a, b). As follows from the experimental data, the variation of corrosion currents with the amount of Nafion® is non-monotonic both for Vulcan XC-72, and for AB.

In order to compare the influence of Nafion® on the corrosion of different materials, currents after 100 s (j_{100}) and 3600 s (j_{3600}) of electrolysis are plotted in Fig. 3 as a function of the Nafion® loading. We applied a formalistic approach, and normalized the mass of ionomer to A_{BET} for pristine carbon materials. As one may see, j_{100} and j_{3600} for Vulcan XC-72 and for AB obey similar inverted volcano-like dependence, with a shallow minimum between 0.5 and 1.2 $mg_{Nafion}\ m_C^{-2}$. However, for T-900 the current is scaling down monotonically. Note that for Vulcan XC-72 1.0 $mg_{Nafion}\ m_C^{-2}$ corresponds to ca. 15 wt% of Nafion® which is comparable to the ionomer content in the catalytic layers of the PEMFCs.

In order to rationalize the observed influence of Nafion® on the corrosion of carbons, it is essential to understand how ionomer molecules are distributed in their pore network. Despite their importance for the performance of the PEMFCs, studies on the interaction of carbon materials with ionomers are not numerous. The most systematic studies were performed by Uchida et al. [27–31] who explored the influence of (i) the carbon support porosity,

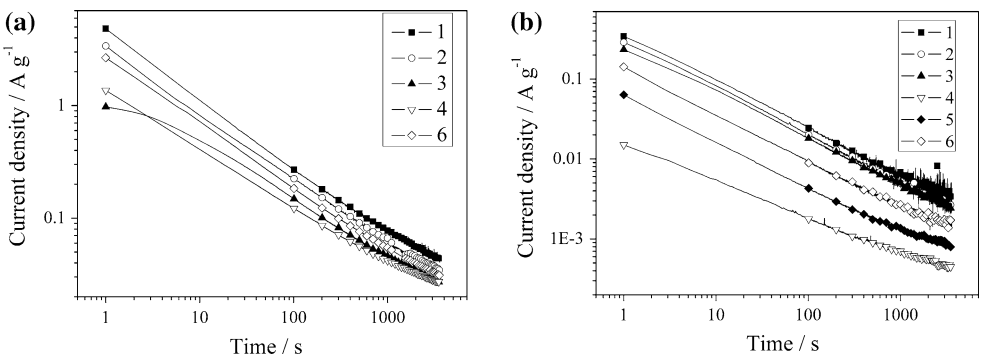

Fig. 1 Chronoamperogramms of Vulcan XC-72 (**a**) and Acetylene black (**b**) oxidation in 2 M H_2SO_4 at 1.1 V vs. RHE. Carbon blacks are impregnated with (1) 0; (2) 0.16; (3) 0.20; (4) 0.79; (5) 1.56; and (6) 3.13 mg Nafion® per m_C^{-2}. Note that *symbols* do not correspond to the actual data points

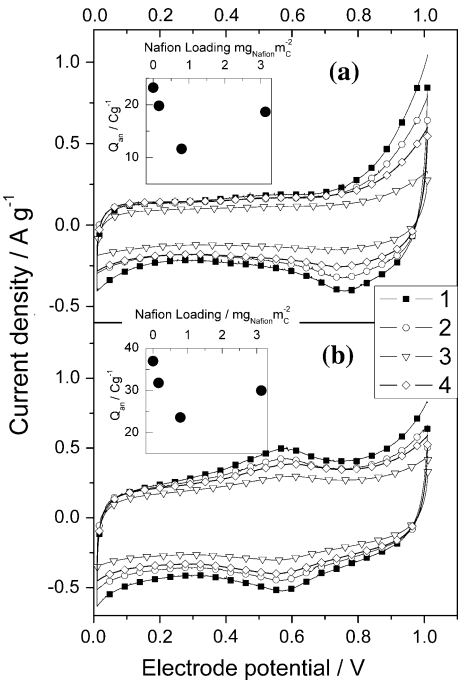

Fig. 2 Cyclic voltamogramms measured at 0.01 V s^{-1} in 2 M H_2SO_4 **a** before electrooxidation and **b** after electrooxidation for Vulcan XC-72 impregnated with different amounts of Nafion®: (1) 0; (2) 0.16; (3) 0.79; (4) 3.13 mg_{Nafion} m_C^{-2},. Note that *symbols* do not correspond to the actual data points. The inserts show the charge of the anodic scans versus the Nafion loading

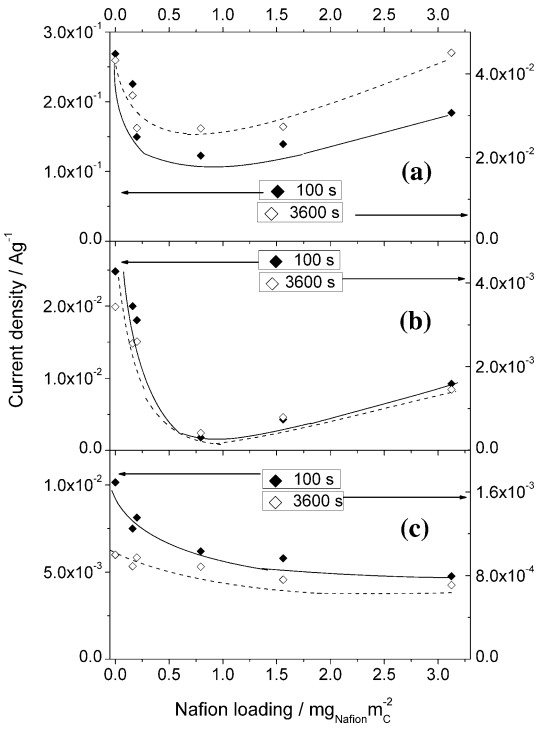

Fig. 3 Dependence of corrosion current at 100 (*filled symbols*) and 3600 s (*open symbols*) on the Nafion® loading for **a** Vulcan XC-72, **b** Acetylene Black, **c** T-900

(ii) the procedure employed for the preparation of the catalyst layers, and (iii) the amount of ionomer on the performance of a PEMFC. Based on the mercury porosimetry study of membrane-electrode assemblies prepared from different carbon materials and various amounts of Flemion® ionomer, they concluded that the ionomer molecules occupied 0.04–1.0 μm pores between carbon agglomerates (named "secondary pores" by Watanabe et al. [32]) and did not penetrate into 0.02–0.04 μm pores between primary carbon particles (named "primary pores" [32]). The authors suggested that ca. 40 nm size colloidal particles of Flemion® could not penetrate pores with the diameter below 40 nm.

Recently Zawodzinski et al. [33] arrived at a somewhat different conclusion. Based on the mercury porosimetry of the membrane-electrode assemblies prepared from Vulcan XC-72 with various amounts of Nafion®, they concluded that the smaller pores (3.5–17 nm in diameter) are filled or blocked by the ionomer, and suggested that in polar solvents the latter exists in the form of rod-like particles with the size between 1.5 and 2.5 nm depending on the ionomer nature and the type of the solvent.

In this study, we employed low temperature nitrogen adsorption for examining the porous structure of carbon blacks impregnated with various amounts of Nafion® ionomer. Compared to the mercury porosimetry, this method has an advantage of applying no deformation on the carbon black aggregates, but it only allows the analysis of micro- and mesopores with the size below 100–300 nm.

We start our discussion by considering the changes of the textural characteristics for Vulcan XC-72, which has the highest BET surface area and thus shows the most significant changes upon impregnation with Nafion® (Table 1). First of all, A_{BET} drops already at 0.16 mg_{Nafion} m_C^{-2} (corresponding to only 3.55 wt% of Nafion®), and then decreases gradually as the loading of the ionomer is increased. This goes along with the decrease of the micropore volume V_μ, and the volume of mesopores in the interval 2 nm $\leq d \leq$ 10 nm calculated as $V_{0.8} - V_\mu$. This finding suggests that both the micropores and small mesopores are either filled or blocked by ionomer molecules. Considering the size of the ionomer molecules, filling of micropores is rather unlikely. Preferential adsorption of the ionomer at micro/mesopore mouths can be explained by higher adsorption potential of structural defects and by retention of the solvent in the small pores by capillary forces upon drying of the samples impregnated with the Nafion®.

It is interesting to note that decrease of the volume of the pores with the size below 10 nm goes with the increase of the volume of mesopores in the interval 10 nm $\leq d \leq$ 300 nm calculated as ($V_\Sigma - V_{0.8}$), and an increase of the mean pore size D_{BET} and D_{BJH}. These changes can be attributed to the effect Nafion® adsorption exerts on the

structure of carbon aggregates. The morphology of carbon black aggregates is characterized by the DBPA number [34]. The so-called "high-structure" carbons are composed of branched aggregates of carbon globules, and are characterized by high (up to ca. 300 cm^3/100 g) DBPA numbers. The "low-structure" carbon blacks with non-aggregated carbon globules have DBPA numbers close to 40 cm^3/100 g. Vulcan XC-72 is a high-structure carbon (see DBPA number in the Table 1) comprising highly branched dendrite-like aggregates composed of interconnected primary particles. Such carbon materials swell when immersed in solvents, and that is what happens during the ink preparation. The higher the surface area of carbon [35, 36], and the more disordered its crystalline structure [36], the larger is the extent of swelling. While such swelling is reversible in pure solvents, it will become irreversible as Nafion® adsorbs at the micropore mouths and in mesopores. Hence, after drying these carbon–Nafion® composites will have deformed structure with larger volume (V_{BJH}), but constant surface area (A_{BJH}) of mesopores. And, this is exactly what we observe for Vulcan XC-72 (Table 1). Deformation induces strain, primarily in the contact areas between carbon particles, resulting in an increase of corrosion currents.

If our reasoning is correct, similar behavior must be observed for other high-structure carbons. Indeed, AB shows similar dependence of corrosion currents on the ionomer loading. The textural characteristics also obey similar trend (Table 1), although the extent of the changes is much smaller in accord with the smaller surface area of AB. Thus, A_{BET} slightly decreases, V_{BJH}, D_{BET}, and D_{BJH} increase, while A_{BJH} remains constant.

Thus, impregnation of carbon blacks with the ionomer produces two counteracting effects: (i) its adsorption on the surface of carbon, leading to the surface blocking and decrease of corrosion currents, and (ii) structural deformation of carbon aggregates resulting in the increase of corrosion currents. Surface blockage by adsorbed Nafion® has been described in a number of publications, e.g. for glassy carbon [37], Pt [38, 39], carbon supported Pt [40], and Au electrodes [39]. Maruyama et al. [37] attributed suppression of the double layer splitting of glassy carbon to the surface blocking by the hydrophobic perfluorocarbon fragments of Nafion®. We studied Nafion® adsorption on various carbon materials from water:isopropanol (1:1) solution and found the monolayer adsorption capacity of ca. 0.28, and 0.85 mg m^{-2} for Vulcan XC-72 and AB, respectively. These values correspond fairly well to those reported by Ma et al. [41] for adsorption from aqueous solutions. The results of the adsorption study will be reported in a separate publication.

Analysis of the electrochemical and N_2 adsorption data suggests that corrosion suppression is not directly related to the pore blocking but is rather connected to the adsorption capacity of carbon materials. Indeed, the strongest suppression is observed for AB (Fig. 3), which contrary to Vulcan XC-72 does not exhibit significant blocking of the pores below 10 nm (Table 1), but whose monolayer adsorption capacity is significantly higher than that for Vulcan XC-72. The higher monolayer adsorption may be related to the more ordered structure of AB (cf. d_{002}, L_c and L_a values for AB and Vulcan XC-72 in the Table 1).

Note that the magnitude of the changes produced by Nafion® adsorption and pore blocking/filling varies in the course of corrosion (Fig. 3). This observation suggests that the interaction of carbons with Nafion® is affected by the electrode potential and/or their surface properties (e.g. presence of functional groups) as inferred earlier in reference [37].

The second phenomenon, namely, deformation of carbon aggregates, is expected to increase as the amount of Nafion® exceeds monolayer adsorption. It is thus likely that the increase of corrosion currents for Vulcan and AB at high Nafion® loadings is due to the described distortion of carbon aggregates. Swelling and deformation of carbon aggregates upon impregnation with Nafion® will produce microstrains in the body of carbon black, especially in the contact areas between the interconnected primary particles. Structural imperfections, located in these regions, then act as the active sites for corrosion attack.

If the above hypothesis is correct, corrosion currents for low-structure carbon materials are expected to decay monotonically with the amount of ionomer. In order to verify this, we tested low-structure T-900 sample with DBPA number 43, whose morphology is quite different from that of Vulcan XC-72 or AB. And indeed, T-900 conforms to the expected behavior (Fig. 3). Moreover, an increase of V_{BJH}, D_{BET} and D_{BJH}, observed for Vulcan XC-72 and AB, which according to our hypothesis is the fingerprint of the aggregate deformation, has not been observed for T-900.

Figure 4 illustrates schematically the phenomena discussed in this study. (1) Carbon black aggregates swell when soaked in a solvent (this happens during the catalyst "ink" preparation), and this results in the increase of the pore volume. (2) Nafion®macromolecules adsorb at structural defects. (3) If the loading of Nafion® is small (A), carbon globules relax to the original structure upon drying. Corrosion of such composite material is slower than that of the pristine carbon black, since Nafion® blocks the surface sites most susceptible to the corrosion attack, in particular in the contact points of primary particles. (4) If the amount of Nafion® in the ink is large (B), drying of the ink results in the condensation of some Nafion® macromolecules in the pores between primary carbon particles. (5) This prevents structural relaxation, and after drying carbon aggregates retain their deformed expanded shape. The

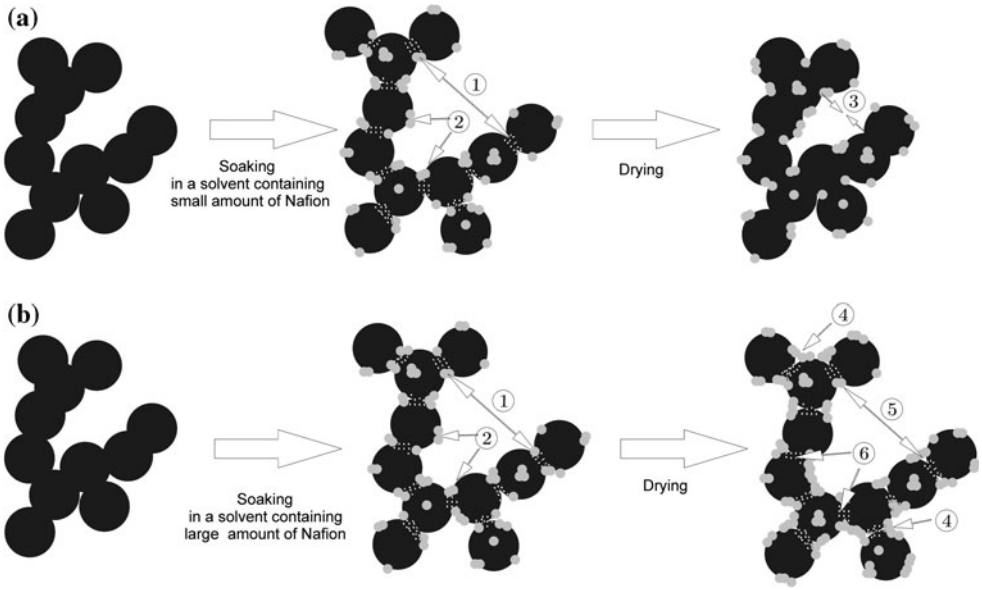

Fig. 4 Schematic representation of the interaction of ionomer macromolecules with high-structure carbon blacks. See text for details

volume of small mesopores decreases not only because of their blocking with polymer molecules, but also because of their transformation into larger mesopores. Simultaneously, the volume of large mesopores increases. (6) Deformation of carbon aggregates leads to initiation of microstrain in the contact areas between interconnected primary carbon particles. Electrochemical corrosion in the strained zones (marked with white spots) is accelerated. While the (A) scenario is possible both for low- and high-structure carbon blacks, the (B) scenario can only be realized for high-structure carbons. Hence, the difference in the behavior of Vulcan XC-72 and AB on the one hand and T-900 on the other hand. Corrosion attack in the contact areas between primary particles may explain the thinning of cathode layers of PEM fuel cells which occurs already at 5–10% loss of the cathode mass.

4 Conclusions

Analysis of the electrochemical and the nitrogen adsorption data suggests that Nafion® adsorbs on the surface of carbon blacks, blocks micropores, blocks or fills small mesopores, and, at high loadings, leads to deformation of carbon aggregates for high-structure carbon blacks. These phenomena strongly influence the rate of the electrochemical corrosion of carbon black materials. The extent of the influence varies depending on the porosity, the aggregate morphology, and the crystallinity of carbon materials.

Since Nafion® is an essential component of the state of the art catalytic layers for the PEM fuel cells, the knowledge of its influence is important for mitigating the degradation processes of the membrane-electrode assemblies. Further studies are required to better understand the interaction of Nafion with carbon materials, and to clarify how an ionomer is distributed on their surface and in the pore volume.

Acknowledgments The authors thank S.V. Cherepanova for the XRD study. Financial support by the Russian Foundation for Basic Research (RFBR) under grant No. 06-03-32737, Russian Federal Agency for Science and Innovations under contract No.02.740.11.5084, and from ANR (France) under grant number ANR-06-CEXC-004 is gratefully acknowledged.

References

1. Vielstich W, Lamm A, Gasteiger HA (eds) (2003) Handbook of fuel cells: fundamentals, technology and applications. Wiley, Chichester
2. Kinoshita K, Bett JAS (1973) Carbon 11:237
3. Stonehart P (1984) Carbon 22:423
4. Antonucci PL, Romeo F, Minutoli M, Alderucci E, Giordano N (1988) Carbon 26:197
5. Antonucci PL, Pino L, Giordano N, Pinna G (1989) Mater Chem Phys 21:495
6. Kinoshita K (1988) Carbon, electrochemical and physicochemical properties. Wiley, New York
7. Giordano N, Antonucci PL, Passalacqua E, Pino L, Arico AS, Kinoshita K (1991) Electrochim Acta 36:1931
8. Willsau J, Heitbaum J (1984) J Electroanal Chem 161:93
9. Tomantschger K, Findlay R, Hanson M, Kordesch K, Srinivasan S (1992) J Power Sources 39:21
10. Wang X, Li W, Chen Z, Waje M, Yan Y (2006) J Power Sources 158:154
11. Li L, Xing Y (2008) J Power Sources 178:75
12. Wang J, Yin G, Shao Y, Zhang S, Wang Z, Gao Y (2007) J Power Sources 171:331
13. Maass S, Finsterwalder F, Frank G, Hartmann R, Merten C (2008) J Power Sources 176:444
14. Oh H, Oh J, Haam S, Arunabha K, Roh B, Hwang I, Kim H (2008) Electrochem Commun 10:1048

15. Wang J, Yin G, Shao Y, Wang Z, Gao Y (2008) J Power Sources 176:128
16. Siroma Z, Ishii K, Yasuda K, Miyazaki Y, Inaba M, Tasaka A (2005) Electrochem Commun 7:1153
17. Li L, Xing Y (2006) J Electrochem Soc 153:A1823
18. Jiang R, Kunz HR, Fenton JM (2006) Electrochim Acta 51:5596
19. Neffe S (1988) Carbon 26:687
20. Colmenares LC, Wurth A, Jusys Z, Behm RJ (2009) J Power Sources 190:14
21. Kangasniemi KH, Condit DA, Jarvi TD (2004) J Electrochem Soc 151:E125
22. Li W, Lane AM (2009) Electrochem Commun 11:1187
23. Karnaukhov AP, Fenelonov VB, VYu Gavrilov (1989) Pure Appl Chem 61:1913
24. Gregg SJ, Sing KSW (1982) Adsorption, surface area and porosity, 2nd edn. Academic Press, London
25. Barrett EP, Joyner LG, Halenda PP (1951) J Am Chem Soc 73:373
26. Reshetenko TV, Avdeeva LB, Ismagilov ZR, Pushkarev VV, Cherepanova SV, Chuvilin AL, Likholobov VA (2003) Carbon 41:1605
27. Uchida M, Fukuoka Y, Sugawara Y, Eda N, Ohta A (1996) J Electrochem Soc 143:2245
28. Uchida M, Aoyama Y, Eda N, Ohta A (1995) J Electrochem Soc 142:4143
29. Uchida M, Fukuoka Y, Sugawara Y, Ohara H, Ohta A (1998) J Electrochem Soc 145:3708
30. Uchida M, Aoyama Y, Tanabe M, Yanagihara N, Eda N, Ohta A (1995) J Electrochem Soc 142:2572
31. Uchida M, Aoyama Y, Eda N, Ohta A (1995) J Electrochem Soc 142:463
32. Watanabe M, Tomikawa M, Motoo S (1985) J Electroanal Chem 195:81
33. Xie J, More KL, ThA Zawodzinski, Smith WH (2004) Electrochem Soc 151:A1841
34. Donnet JB, Bansal RC, Wang MJ (eds) (1993) Carbon black, 2nd edn. Marcel Dekker, New York
35. Serpinskii VV, Yakubov TS (1981) Russ Chem Bull 54
36. Romanenko AV, Simonov PA (2004) CarboCat-2004. In: 1st International symposium on carbon for catalysis, 18–20 July 2004, Lausanne, Switzerland, p 111 (Book of abstracts)
37. Maruyama J, Abe I (2001) Electrochim Acta 46:3381
38. Gottesfeld S, Raistrick ID, Srinivasan S (1987) J Electrochem Soc 134:1455
39. Chu D, Tryk D, Gervasio D, Yeager EB (1989) J Electroanal Chem 272:277
40. Ignaszak A, Ye S, Gyenge E (2009) J Phys Chem C 113:298
41. Ma Sh, Chen Q, Jøgensen FH, Stein PC, Skou EM (2007) Solid State Ionics 178:1568